Supplemental Information

Supplemental Materials and Methods

Sample preparation and karyotyping

Fetal livers were removed from embryos by dissection. Samples were homogenized by pipetting and passage through a 70 μm cell strainer, frozen in FBS + 5% dimethylsulfoxide and stored in liquid nitrogen. For *Bub1b*$^{H/H}$ embryos and adult mice, tissue samples were sent to Transnetyx (Cordova, TN) for genotyping using the protocol described previously (Baker et al. 2004). For trisomic embryos, mouse embryonic fibroblasts (MEFs) were derived, and karyotype was determined by metaphase spreads of MEFs as described previously (Williams et al. 2008). Karytoype was confirmed by qPCR of genomic DNA derived from MEF cell pellets. Briefly, cells were digested 4-16 hours at 55^{o}C in 10 mM Tris pH 8.0, 100 mM NaCl, 10 mM EDTA pH 8.0, 0.5% SDS solution with 0.4 mg/ml proteinase K. Genomic DNA was precipitated with isopropanol, washed with 70% ethanol, resuspended in double deionized water, and incubated at 95^{o}C for 5 minutes. qPCR was performed on DNA samples by mixing Takara SYBR *Premix Ex Taq II* (Tli RNase H Plus, ClonTech, Mountain View, CA) master mix with the primers described in Supplemental Table 1, and amplified using a LightCycler 480 II (Roche). Samples were normalized to the copy number-invariant reference gene *Glucagon* (GCG) as described (Ballester et al. 2013). Genes amplified were selected based on low propensity for copy number variation (She et al. 2008) and chromosomal location, and primers were designed to amplify across intron-exon boundaries.

Homing assays

Recipient mice for homing assays were irradiated with 8.5 Gy administered as a single dose. After thawing, fetal liver cells were labeled with CM-DiI (Life Technologies) according to the manufacturer's instructions, and then evaluated for degree of labeling and viability by propidium iodide exclusion with an LSR II flow cytometer (Becton Dickinson). 2x10^{6} live cells were

injected intravenously, and bone marrow was harvested by flushing the long bones 24 hours after injection. Red blood cells were lysed in ACK Lysing Buffer, samples were washed in IMDM containing 2% FBS, then the proportion of labeled cells in the bone marrow was evaluated on an LSR II flow cytometer (Becton Dickinson). Three trisomy 19 fetal livers were pooled for homing assays due to low fetal liver cell recovery from these embryos.

Single cell sequencing

Peripheral blood was collected from CD45.1 recipient mice reconstituted with fetal liver cells isolated from E14.5 *Bub1b*$^{H/H}$ embryos and a common euploid CD45.1 donor, from mice reconstituted with E14.5 *Bub1b*$^{H/H}$ fetal liver cells alone or from mice reconstituted with bone marrow cells from 6- to 12-week old adult mice. Blood was processed as described in the Methods, and *Bub1b*$^{H/H}$ white blood cells were sorted using a MoFlo cell sorter (Beckman-Coulter) or Aria I cell sorter (Beckson Dickinson). *Bub1b*$^{H/H}$ cells were sorted using a CD45.2 antibody, and CD45.1 recipient-derived cells were excluded using a CD45.1 antibody (Biolegend).

To isolate BM-HSCs, bone marrow cells were isolated as described for bone marrow transfers. White blood cells were counted before the bone marrow was incubated at an appropriate concentration in antibodies detecting CD150, CD48, CD117, Sca-1 (from BioLegend) and a mouse lineage antibody cocktail labeled with biotin obtained from Miltenyi Biotech. Cells were subsequently incubated with anti-biotin microbeads, then differentiated cells were depleted from the cell suspension by retention of biotin-positive cells on a MACS column (Miltenyi Biotech). Lineage-depleted cell suspensions were then double sorted on a FACSAria II cell sorter (Becton Dickinson), first for lineage negative, CD48 negative cells, then for lineage negative, CD48 negative, CD150 positive, CD117 positive, Sca-1 positive cells. FL-HSCs were

isolated in the same manner, except using the markers and lineage cocktail described in the Methods for HSC quantification.

Keratinocytes were isolated from the backskin of a 4-month old *Bub1b*$^{H/H}$ mouse. Hair was plucked from the backskin, then the backskin was digested in 0.25% trypsin in PBS overnight at 4^{o}C. The epidermis was removed from the underlying dermis using forceps, then transferred to DMEM containing 10% FBS and minced with a razor blade. The minced dermis was then both sedimented and passed through a 70 μm cell strainer twice. The pellet was again passed through a 70 μm cell strainer before isolation by microaspiration.

Intestinal crypt cells were isolated from a 4-month old *Bub1b*$^{H/H}$ mouse as described previously (Yilmaz et al. 2012). Briefly, the small intestines were dissected and the fat and mesentery was removed. The intestinal lumen was washed thoroughly with ice cold PBS using a 20G feeding needle. The intestines were then opened longitudinally, and the mucus was removed by gently rubbing the intestines in cold PBS. The intestines were then cut into small pieces and washed further in ice cold PBS with occasional shaking. The pieces were then incubated and washed three times in ice cold PBS/EDTA (10 mM) with occasional shaking before trituration with a pipette then passage through a 70 μm cell strainer. The resulting cell suspension was greatly enriched for crypt cells as assessed by visual inspection under a microscope. To liberate cells from the crypts, the cell suspension was concentrated by centrifugation, resuspended in TrypLE Express (Thermo Fisher) and incubated for 1 minute at 37^{o}C, then placed on ice. S-MEM was added, then the cells was concentrated by centrifugation before dilution in S-MEM for isolation by microaspiration.

All single cells were isolated after appropriate preparation by microaspiration, and then amplified, sequenced and analyzed as described (Knouse et al. 2014).

Quantification of trisomic fetal liver area
Embryos were isolated at embryonic day E14.5 and fixed overnight in Bouin's solution. Embryos were sectioned into 5 μm slices and stained with hematoxylin and eosin. Slides were then scanned on a Leica Aperio slide scanner, and fetal liver area was measured using ImageJ.

Quantification of relative fetal liver cell recovery
Fetal livers were preserved and then thawed as described above. Cell number was counted in triplicate using a Cellometer Auto T4 cell counter (Nexelcom).

Supplemental References

Ballester M, Castelló A, Ramayo-Caldas Y, Folch JM. 2013. A quantitative real-time PCR method using an X-linked gene for sex typing in pigs. *Mol Biotechnol* **54**: 493–496.

She X, Cheng Z, Zöllner S, Church DM, Eichler EE. 2008. Mouse segmental duplication and copy number variation. *Nature Genetics* **40**: 909–914.

Yilmaz OH, Katajisto P, Lamming DW, Gültekin Y, Bauer-Rowe KE, Sengupta S, Birsoy K, Dursun A, Yilmaz VO, Selig M, et al. 2012. mTORC1 in the Paneth cell niche couples intestinal stem-cell function to calorie intake. *Nature* **486**: 490–495.

Supplemental Figure Legends

Supplemental Figure 1. *Evaluation of trisomic fetal livers*
Representative image of sagittal cross section of fetal livers from E14.5 WT (A) or trisomy 19 (B) embryos. (C) Quantification of trisomic fetal liver cross section area relative to cross section area of wild type littermate. (D) Relative recovery of trisomy 16, trisomy 19 and $Bub1b^{H/H}$ E14.5 fetal liver cells compared to wild type littermates after cryo-preservation and thawing. Data are shown as mean ± SD.

Supplemental Figure 2. *Peripheral blood analyses of trisomy 16 primary recipients*
Flow cytometry of peripheral blood from trisomy 16 and wild type primary recipients was performed to quantify the percentage of B220-positive B cells (A) and Thy1.2-positive T cells (B) in the peripheral blood. Complete blood cell counts of peripheral blood from trisomy 16 and wild type primary recipients was performed to determine red blood cell count (C), mean corpuscular volume (MCV) (D), mean corpuscular hemoglobin (MCH) (E), mean corpuscular hemoglobin concentration (MCHC) (F), hemoglobin content (G) and platelet counts (H). The composition of the leukocyte population was evaluated by automated differential for trisomy 16 and wild type primary recipients (I). In all graphs, the bars represent the mean value for each time point and condition, and asterisks indicate the trisomy 16 values are significantly different from the values of wild type littermates at the indicated time by t-test ($p<0.05$). (J) Plots of red blood cell number versus mean corpuscular volume (MCV) of all trisomy 16 primary recipients and wild type primary recipients at all times evaluated above. (K) Quantification of the percentage of $CD150^+$, $Sca\text{-}1^+$, $CD117^+$, $CD48^-$ cells in the bone marrow of trisomy 16 and wild type primary recipients at 25 weeks post-transplantation. Data are represented as mean ± SD.

Supplemental Figure 3. *Peripheral blood analyses of trisomy 19 primary and secondary recipients*
Flow cytometry of peripheral blood from trisomy 19 and wild type primary recipients was performed to quantify the percentage B220-positive B cells (A) and Thy1.2-positive T cells (B) in the peripheral blood. Complete blood cell counts of peripheral blood from trisomy 19 and wild type primary recipients was performed to determine red blood cell counts (C), mean corpuscular volume (MCV) (D), mean corpuscular hemoglobin (MCH) (E), mean corpuscular hemoglobin concentration (MCHC) (F), hemoglobin content (G) and platelet counts (H). The composition of the leukocyte population was evaluated by automated differential for trisomy 19 and wild type

primary recipients (I). In all graphs, the bars represent the mean value for each time point and condition. (J) Plots of red blood cell number versus mean corpuscular volume (MCV) of all trisomy 19 primary recipients and wild type primary recipients at all times evaluated above. Flow cytometry of peripheral blood from trisomy 19 and wild type secondary recipients was performed to quantify the percentage of B220-positive B cells (K) and Thy1.2-positive T cells (L) in the peripheral blood. Complete blood cell counts of peripheral blood from trisomy 19 and wild type secondary recipients was performed to determine white blood cell counts (M), hematocrit (N), red blood cell counts (O), mean corpuscular volume (MCV) (P), mean corpuscular hemoglobin (MCH) (Q), mean corpuscular hemoglobin concentration (MHCH) (R), hemoglobin content (S) and platelet counts (T). The composition of the leukocyte population was evaluated by automated differential for trisomy 19 and wild type secondary recipients (U). (V) Quantification of the percentage of $CD150^{+}$, $Sca\text{-}1^{+}$, $CD117^{+}$, $CD48^{-}$ cells in the bone marrow of trisomy 19 and wild type secondary recipients at 62 weeks post-transplantation. Data are represented as mean ± SD. In all graphs, the bars represent the mean value for each time point and condition, and asterisks indicate the trisomy 19 values are significantly different from the values of wild type littermates at the indicated time by Student's t-test ($p<0.05$).

Supplemental Figure 4. *Peripheral blood cell and HSC analyses of trisomy 19 tertiary recipients and quaternary recipient survival*
Flow cytometry of peripheral blood from trisomy 19 and wild type tertiary recipients was performed to quantify the percentage of B220-positive B cells (A) and Thy1.2-positive T cells (B) in the peripheral blood. Complete blood cell counts of peripheral blood from trisomy 19 and wild type tertiary recipients was performed to determine white blood cell counts (C), hematocrit (D), red blood cell counts (E), mean corpuscular volume (MCV) (F), mean corpuscular

hemoglobin (MCH) (G), mean corpuscular hemoglobin concentration (MHCH) (H), hemoglobin content (I) and platelet counts (J). The composition of the leukocyte population was evaluated by automated differential for trisomy 19 and wild type tertiary recipients (K). (L) Survival of trisomy 19 and wild type tertiary recipients. (M) Quantification of the percentage of $CD150^{+}$, $Sca\text{-}1^{+}$, $CD117^{+}$, $CD48^{-}$ cells in the bone marrow of trisomy 19 and wild type tertiary recipients at 44 weeks post-transplantation. Data are represented as mean ± SD. (N) Segmentation plots showing the karyotype of CD45.2 peripheral blood cells isolated from two trisomy 19 quaternary recipients (one with high trisomy 19 contribution, one with low trisomy 19 contribution). Segmentation plots show the copy number of all chromosomes from 1 to X relative to a euploid reference on a $\log_2$ scale. Trisomic chromosome is highlighted in red. (O) Survival of trisomy 19 and wild type quaternary recipients. In all graphs, the bars represent the mean value for each time point and condition, and asterisks indicate the trisomy 16 values are significantly different from the values of wild type littermates at the indicated time by t-test ($p<0.05$).

Supplemental Figure 5. *Peripheral blood of adult $Bub1b^{H/H}$ mice is normal and $Bub1b^{H/H}$ adult bone marrow HSCs show no fitness defects in competitive reconstitution assays*
Complete blood cells counts of 12-week old *$Bub1b^{H/H}$* mice and wild type littermate controls: (A) red blood cell count, (B) white blood cell count, (C) mean corpuscular volume (MCV), (D) mean corpuscular hemoglobin (MCH), (E) mean corpuscular hemoglobin concentration (MCHC), (F) hematocrit, (G) hemoglobin content and (H) platelet counts. (I) Quantification of the percentage of $CD150^{+}$, $Sca\text{-}1^{+}$, $CD117^{+}$, $CD48^{-}$ cells in the bone marrow of adult *$Bub1b^{H/H}$* mice and wild type littermates (n=3 for each). Data are represented as mean ± SD. (J-L) CD45.2 *$Bub1b^{H/H}$* (J) or wild type littermate (K) bone marrow cells were co-transferred with an equal number of bone marrow cells from a common CD45.1 donor mouse of the same age into a

lethally irradiated CD45.1 recipient. Peripheral blood was sampled at indicated times and the percentage of the white blood cell population contributed by each donor was quantified by flow cytometry with antibodies against CD45.1 and CD45.2. Data are represented as mean ± SD for each time point. (L) Ratios of the average percentage of the peripheral blood reconstituted by the *Bub1b*$^{H/H}$ bone marrow cells to the average percentage of the peripheral blood reconstituted by wild type littermate bone marrow cells at all indicated times.

Supplemental Figure 6. *Peripheral blood analyses and HSC counts from Bub1b*$^{H/H}$ *bone marrow primary and secondary recipients*
(A-I) Complete blood cell counts of peripheral blood from *Bub1b*$^{H/H}$ and wild type primary bone marrow recipients were performed to determine white blood cell counts (A). Flow cytometry was performed to quantify the percentage B220-positive B cells (B) and Thy1.2-positive T cells (C) in the peripheral blood of primary recipients. Complete blood cell counts further determined red blood cell counts (D), mean corpuscular volume (MCV) (E), hematocrit (F), hemoglobin content (G) and platelet counts (H). The composition of the leukocyte population was evaluated by automated differential for *Bub1b*$^{H/H}$ and wild type primary recipients (I). (J) Quantification of the percentage of CD150^{+}, Sca-1^{+}, CD117^{+}, CD48^{-} cells in the bone marrow of *Bub1b*$^{H/H}$ and *Bub1b*$^{+/H}$ primary recipients 63 weeks post-transplantation. Data are represented as mean ± SD. (K-S) Complete blood cell counts of peripheral blood from *Bub1b*$^{H/H}$ and wild type secondary bone marrow recipients were performed to determine white blood cell counts (K). Flow cytometry was performed to quantify the percentage B220-positive B cells (L) and Thy1.2-positive T cells (M) in the peripheral blood of secondary recipients. Complete blood cell counts further determined hematocrit (N), red blood cell counts (O), mean corpuscular volume (MCV) (P), hemoglobin content (Q) and platelet counts (R). The composition of the leukocyte

population was evaluated by automated differential for *Bub1b*$^{H/H}$ and wild type secondary recipients (S). (T) Quantification of the percentage of CD150^{+}, Sca-1^{+}, CD117^{+}, CD48^{-} cells in the bone marrow of *Bub1b*$^{H/H}$ and wild type secondary recipients at 47 weeks post-transplantation. Data are represented as mean ± SD. In all graphs, the bars represent the mean value for each time point and condition, and asterisks indicate the *Bub1b*$^{H/H}$ values that are significantly different from the values of wild type littermates at the indicated time by t-test ($p<0.05$).

Supplemental Figure 7. *Single cell sequencing analyses of Bub1b*$^{H/H}$ *fetal liver HSCs and peripheral blood cells from a Bub1b*$^{H/H}$ *fetal liver competition assay recipient and a Bub1b*$^{H/H}$ *secondary bone marrow recipient*
Segmentation plots of single cell karyotypes determined by single cell sequencing of CD45.2 positive peripheral blood cells derived from *Bub1b*$^{H/H}$ FL-HSCs from Fig. 1F (A) and from bone marrow HSCs from secondary recipients from Fig. 6A (B). Segmentation plots of single cell karyotypes determined by single cell sequencing of HSCs from *Bub1b*$^{H/H}$ fetal liver (C) or bone marrow (D) from Fig. 6A. Segmentation plots show the copy number of single cells from chromosome 1 to X relative to a euploid reference on a $\log_2$ scale. Segments above the threshold for whole chromosome gain are shown in red, and segments below the threshold for whole chromosome loss are shown in green. Cells that are classified as aneuploid are highlighted with and asterisk on the right.

Supplemental Figure 8. *Single cell sequencing analyses of Bub1b*$^{H/H}$ *fetal liver and bone marrow primary recipients with time*
Segmentation plots of single cell karyotypes determined by single cell sequencing of CD45.2 positive peripheral blood cells derived from *Bub1b*$^{H/H}$ FL-HSCs 3 weeks (A), 6 weeks (B), 13 weeks (C) and 36 weeks (D) after transfer; and of CD45.2 positive peripheral blood cells derived

from *Bub1b*$^{H/H}$ BM-HSCs 3 weeks (E), 6 weeks (F), 13 weeks (G) and 34 weeks (H) after transfer. Segmentation plots show the copy number of single cells from chromosome 1 to X relative to a euploid reference on a $\log_2$ scale. Segments above the threshold for whole chromosome gain are shown in red, and segments below the threshold for whole chromosome loss are shown in green. Cells that are classified as aneuploid are highlighted with and asterisk on the right.

Supplemental Figure 9. *Single cell sequencing analysis of cells from adult Bub1b*$^{H/H}$ *mice*
Segmentation plots of single cell karyotypes determined by single cell sequencing of peripheral white blood cells (A), keratinocytes (B), intestinal crypt cells (C), hepatocyte nuclei (D) and neurons (E) isolated from adult *Bub1b*$^{H/H}$ mice. Segmentation plots show the copy number of single cells from chromosome 1 to X relative to a euploid reference on a $\log_2$ scale. Segments above the threshold for whole chromosome gain are shown in red, and segments below the threshold for whole chromosomes loss are shown in green. Cells that are classified as aneuploid are highlighted with and asterisk on the right.

Supplemental Figure 10. *Frequency of specific chromosome gains and losses in aneuploid Bub1b*$^{H/H}$ *mouse cells*
(A) Plot of frequency of chromosome gain versus frequency of chromosome loss across all sequenced peripheral blood cells after transplantation. (B) Plot of frequency of chromosome gain versus frequency of chromosome loss across all sequenced adult neurons and hepatocytes.

Supplemental Table 1. *Primers used for karyotyping qPCR*

Chromosome	Gene	Forward Primer	Reverse Primer	Source
2	Glucagon (*GCG*)	5'–AACATTGCCAAACGTCATGATG–3'	5'–GCCTTCCTCGGCCTTTCA–3'	Ballester et al., 2013
X	Glycoprotein M6B (*GM6B*)	5'–CTCTTCCACCAGCTGATCTACATG–3'	5'–TCCCGACTCTTAAACTTCAAAACC–3'	Ballester et al., 2013
16	Runt-related transcription factor 1 (*RUNX1*)	5'–CAGGTATACCTTGGATCAGTGC–3'	5'–CAACACAGCATCTTCTGATGGC–3'	This study
16	Eph receptor A3 (*EPHA3*)	5'–AGGAATCATCCCAGCAACACAC–3'	5'–GAGAGCAATCTAGTATTGTTCTGGG–3'	This study
16	Oxysterol binding protein-like 11 (*OSBPL11*)	5'–CCCAATTAAGTGCATACCCAGC–3'	5'–CAAGAGACAGTCAGCAAACACGG–3'	This study
16	Epithelial membrane protein 2 (*EMP2*)	5'–CTCTGTTCTCATGAATGAGCCTG–3'	5'–CAGAAAGAATCGAAGGGAGATTG–3'	This study
19	Bestrophin 1 (*BEST1*)	5'–CAGGGCAGAGGTCATGGTTC–3'	5'–CTGGTGCTCAAGGCAGACCT–3'	This study
19	Ankyrin repeat domain 1 (cardiac muscle) (*ANKRD1*)	5'-GTGCACATGGAAATGACTGG-3'	5'-TGGGCCACAACTCAATGTTA-3'	This study
19	Oligonucleotide/ oligosaccharide-binding fold containing 1 (*OBFC1*)	5'-CTGCACGAAACCTTGCATGA-3'	5'-GCCCCGGCTGATCTTAATCT-3'	This study
19	Caspase 7 (CASP7)	5'–CAATCTGCCACTCTGCAACC–3'	5'–CAGCAACATTGAACAGGCT– 3'	This study

Supplemental Fig. S1

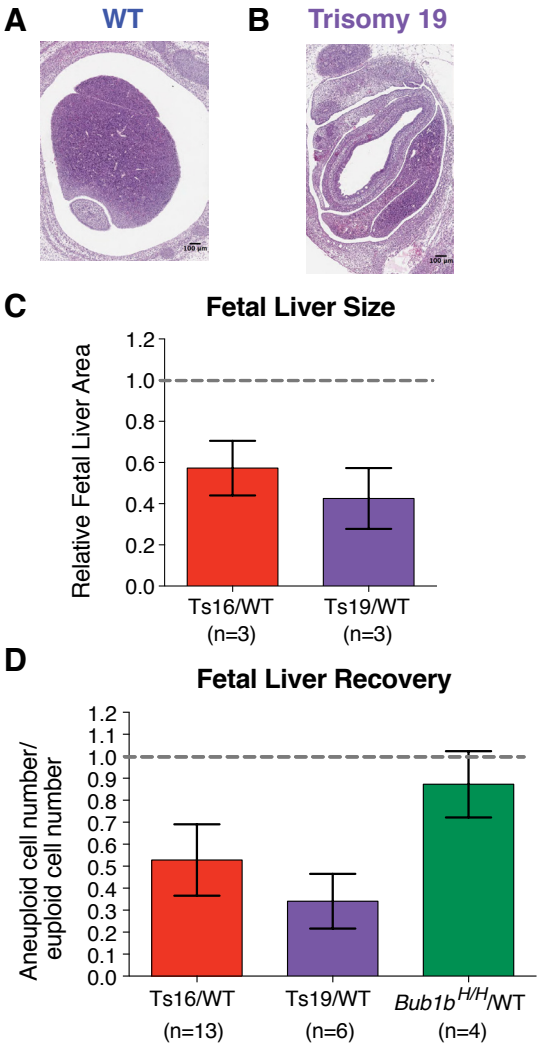

Supplemental Fig. S2

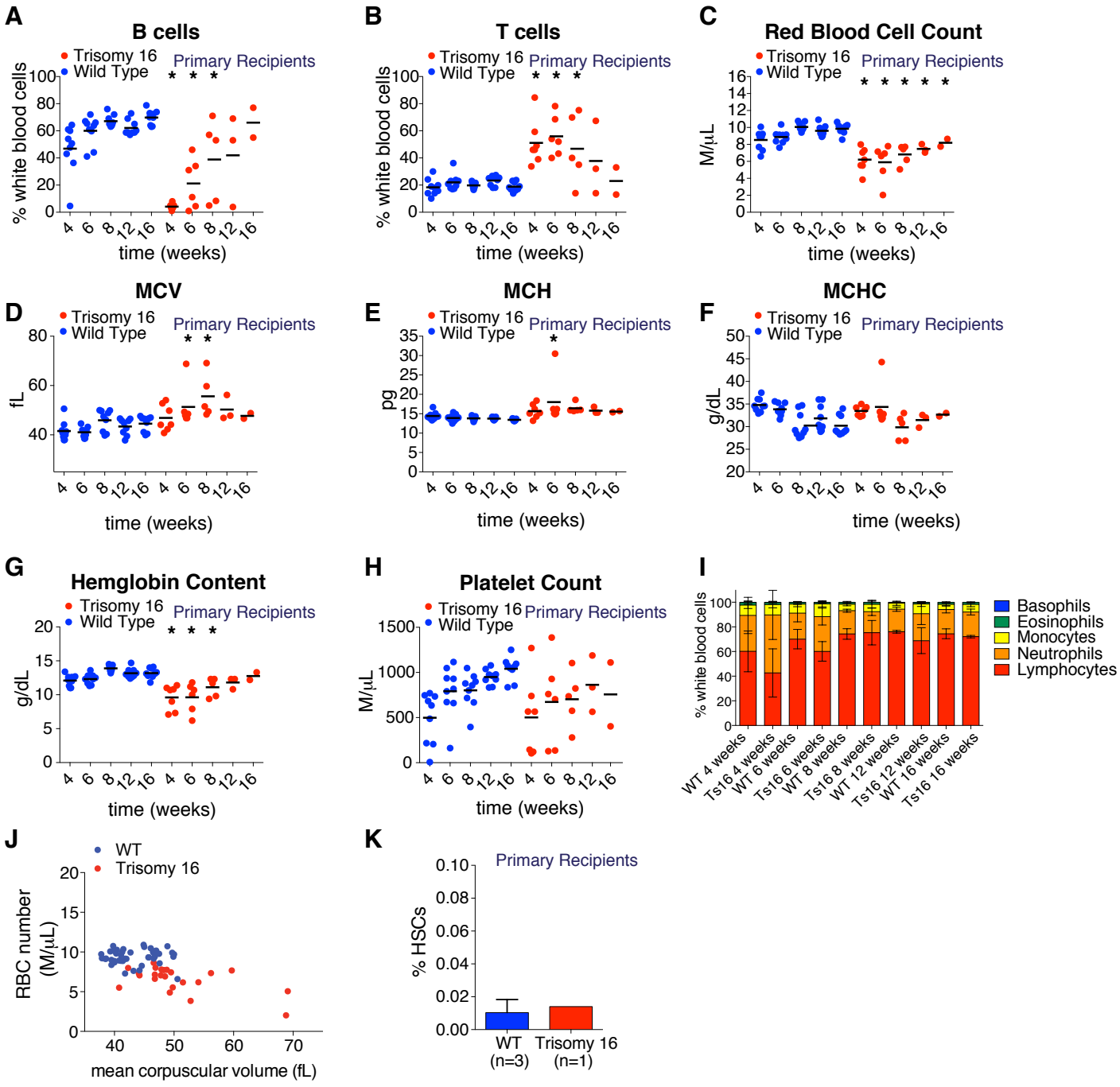

Supplemental Fig. S3

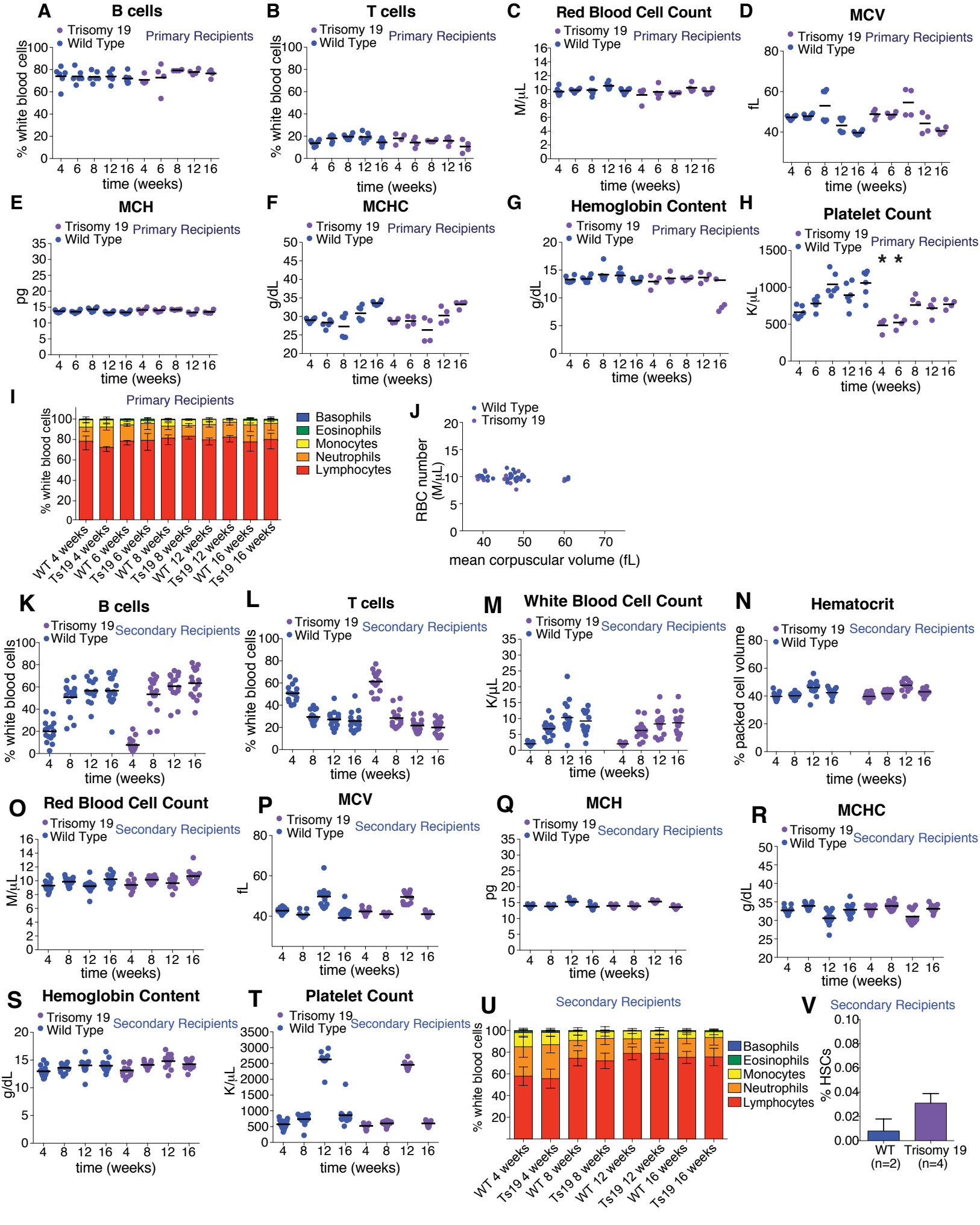

Supplemental Fig. S4

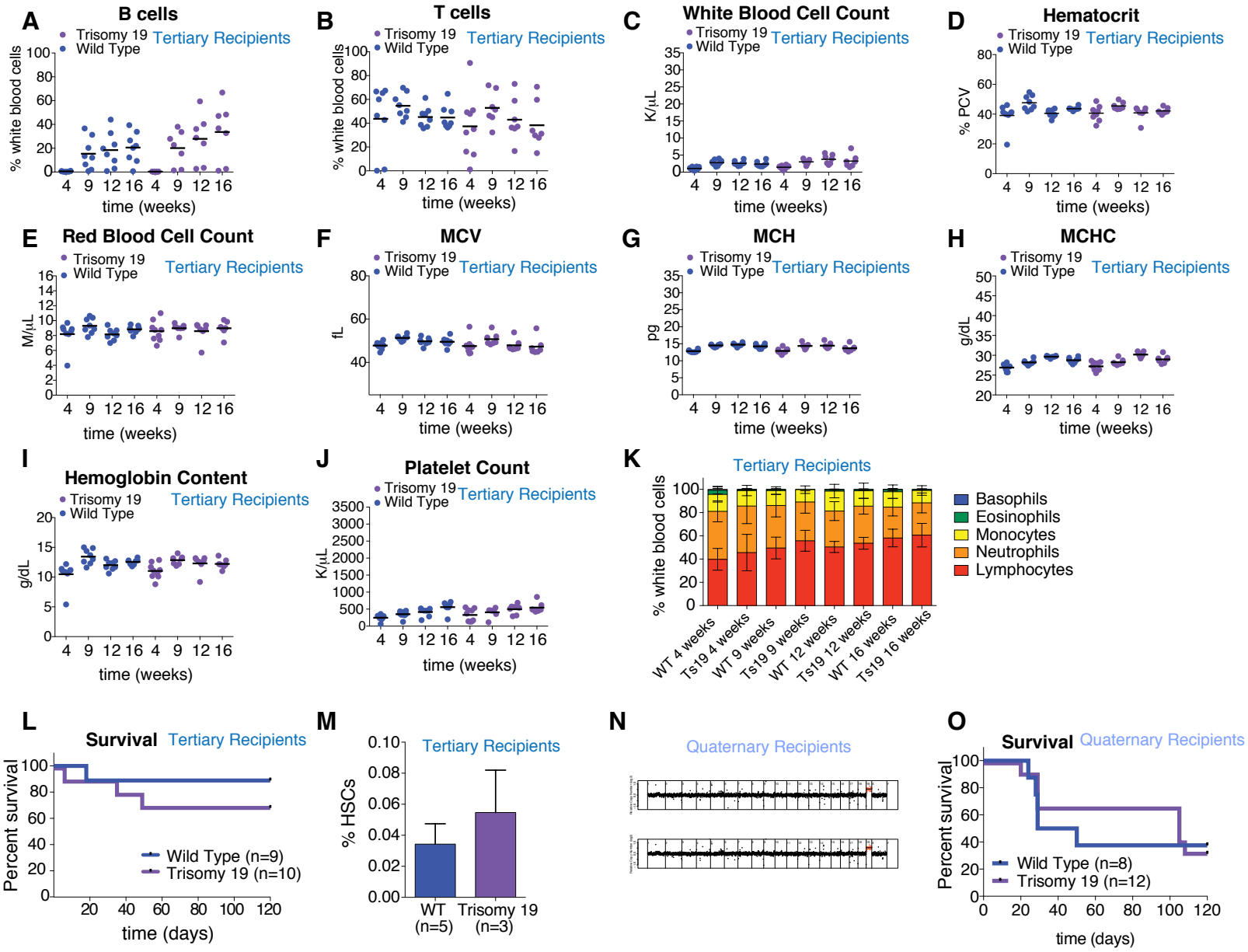

Supplemental Fig. S5

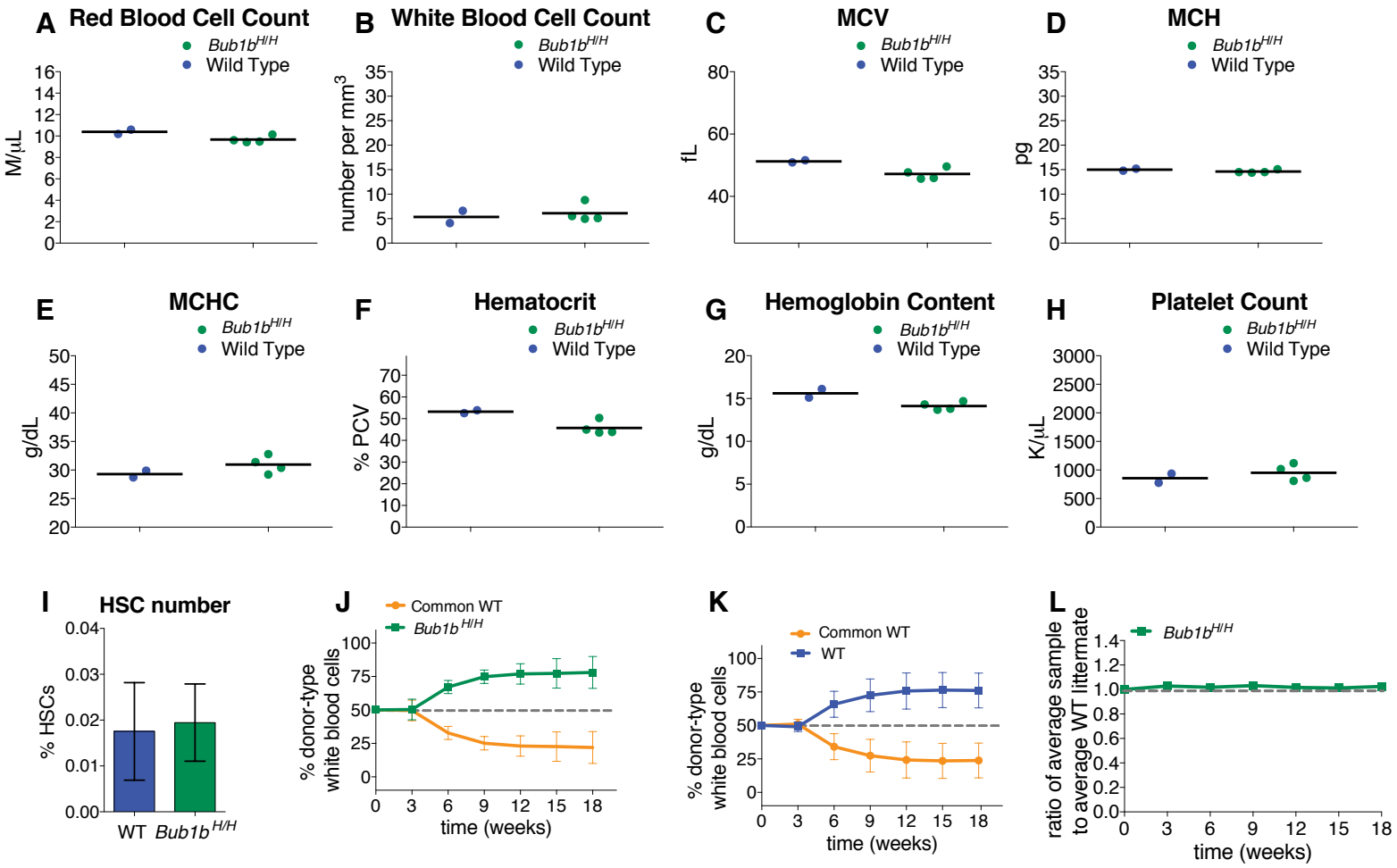

Supplemental Fig. S6

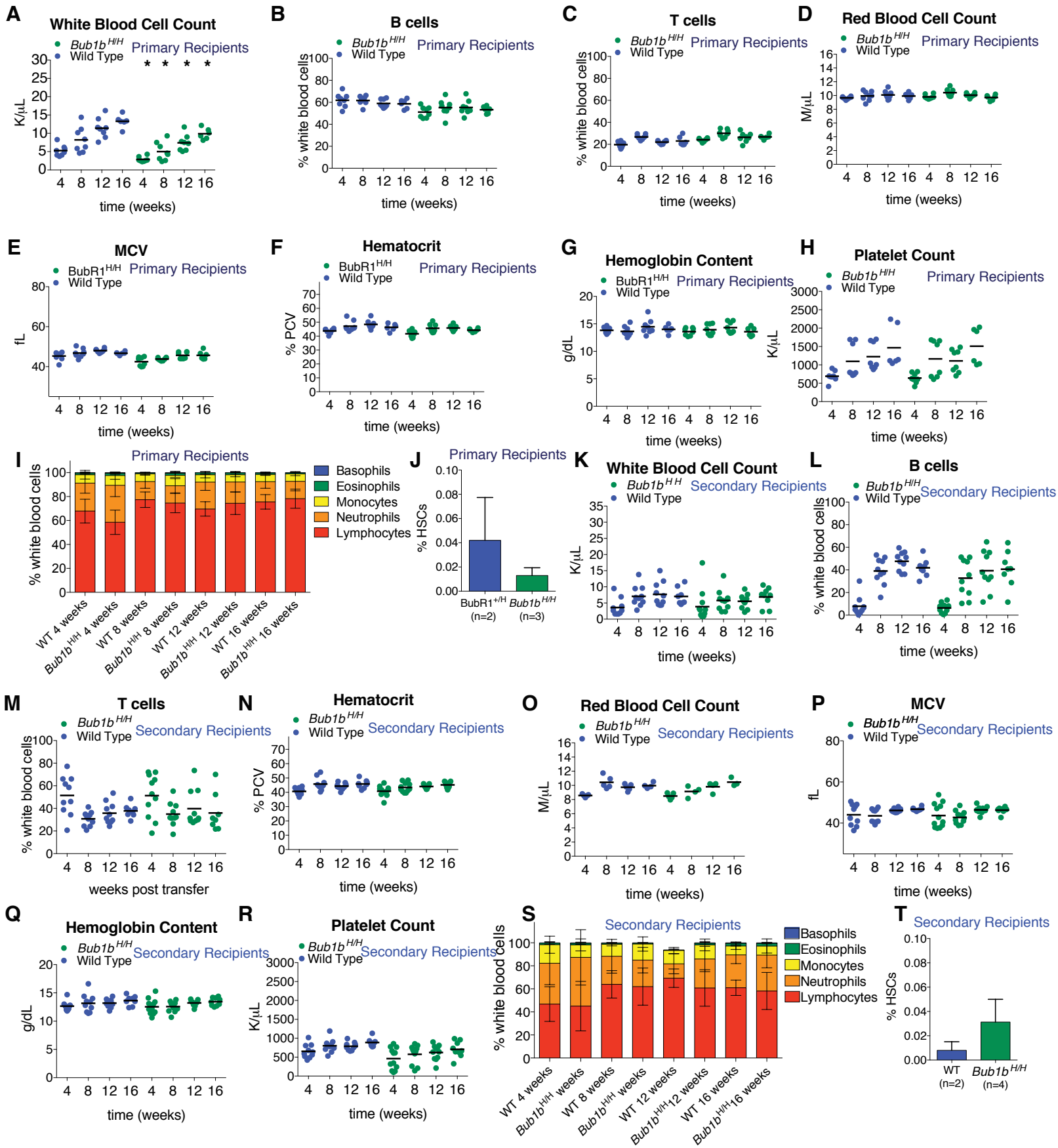

Supplemental Fig. S7

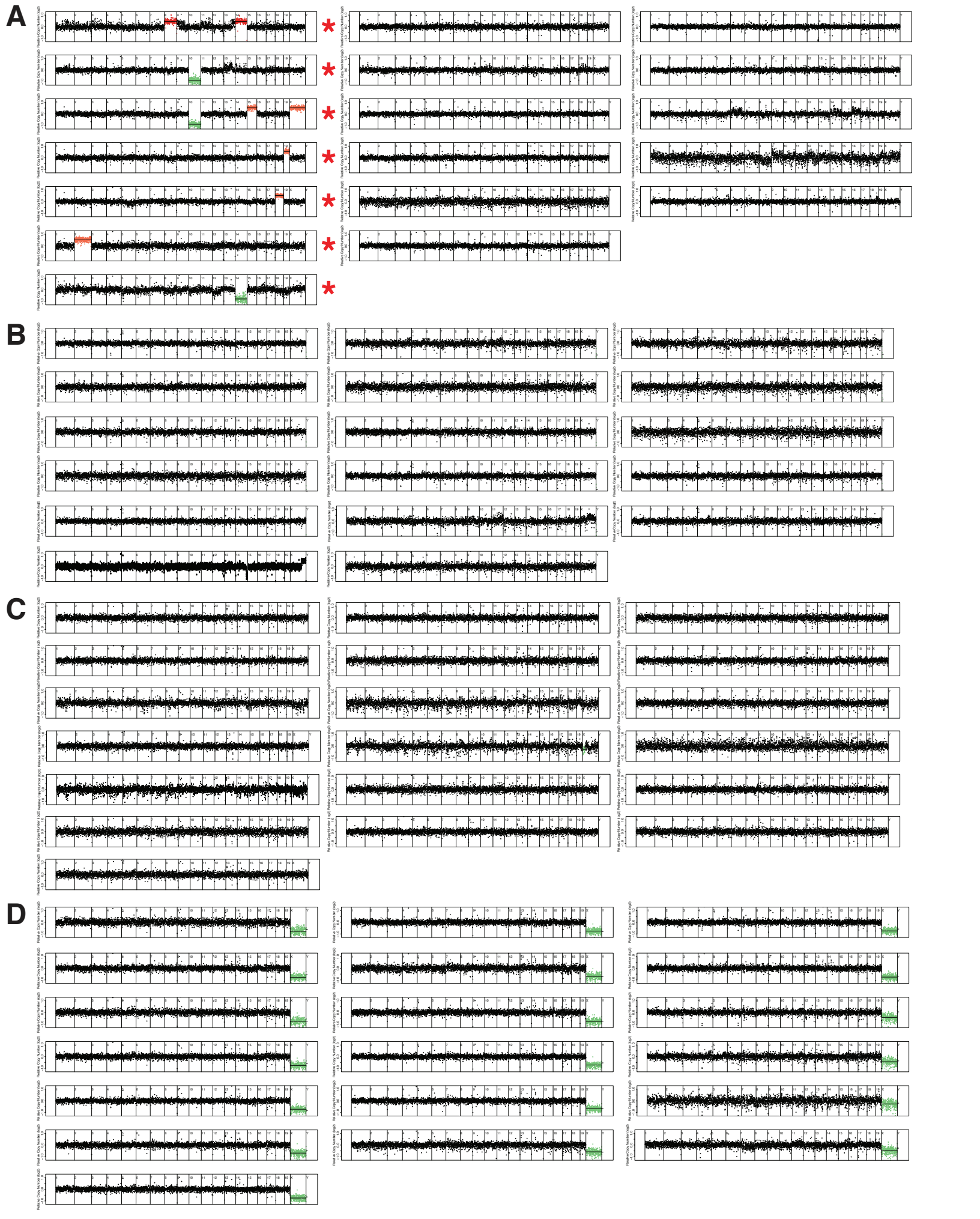

Supplemental Fig. S8